Replacement of Lysine 45 by Uncharged Residues Modulates the Redox-Bohr Effect in Tetraheme Cytochrome c_3 of *Desulfovibrio vulgaris* (Hildenborough)[†]

Lígia M. Saraiva,[‡] Carlos A. Salgueiro,[‡] Patrícia N. da Costa,[‡] Ana C. Messias,[‡] Jean LeGall,[§] Walter M. A. M. van Dongen,[⊥] and António V. Xavier*[,‡]

Instituto de Tecnologia Química e Biológica, Universidade Nova de Lisboa, Apt. 127, 2780 Oeiras, Portugal, Department of Biochemistry and Molecular Biology, University of Georgia, Athens, Georgia 30602, and Department of Biochemistry, Wageningen Agricultural University, Dreijenlaan 3, 6703 HA Wageningen, The Netherlands

Received May 1, 1998; Revised Manuscript Received June 29, 1998

ABSTRACT: The structural basis for the pH dependence of the redox potential in the tetrahemic *Desulfovibrio vulgaris* (Hildenborough) cytochrome c_3 was investigated by site-directed mutagenesis of charged residues in the vicinity of heme I. Mutation of lysine 45, located in the neighborhood of the propionates of heme I, by uncharged residues, namely threonine, glutamine and leucine, was performed. The replacement of a conserved charged residue, aspartate 7, present in the N-terminal region and near heme I was also attempted. The analysis of the redox interactions as well as the redox-Bohr behavior of the mutated cytochromes c_3 allowed the conclusion that residue 45 has a functional role in the control of the pK_a of the propionate groups of heme I and confirms the involvement of this residue in the redox-Bohr effect.

Observed in several electron-transfer proteins, the pH dependence of the redox potential (the redox-Bohr effect) is a mechanism that not only allows a fine regulation of the redox potential but also allows the coupling between electronic and protonic energy, a key process in bioenergetics (*1*−*3*). Several studies have been performed with different cytochromes in order to elucidate the molecular basis responsible for the redox-Bohr effect, suggesting the involvement of heme propionates (*4*−*10*). Although the pK_a of a solvent-exposed propionate group is usually low (p$K_a \sim 4$), insertion of such a group into the hydrophobic core of a protein, incorporation into a hydrogen-bonding network, and/or the presence of charged residues in the immediate environment may significantly increase the pK_a to values which are within the pH range where the redox-Bohr effect is observed in cytochromes.

Tetraheme cytochromes c_3 are small (∼14 kDa), soluble electron-transfer proteins from sulfate reducing bacteria that have been extensively characterized in recent years, both structurally and biochemically (*11*−*14*). In particular, cytochrome c_3 from *Desulfovibrio vulgaris* (Hildenborough) (*Dv*Hc_3)[1] exhibits homotropic (electron/electron) and heterotropic (electron/proton) cooperativities. A detailed analysis of the pH behavior was performed resulting in the following conclusions: (i) the cytochrome has the ability to couple proton transfer with a concerted two-electron transfer (*15*); (ii) two protons participate in this redox-Bohr effect and they titrate with the same pK_a (*16*); (iii) the redox-Bohr cooperativities are all positive since the macroscopic pK_a's of the redox-Bohr protons increase along the reduction process [pK_a's of 5.3, 5.6, 6.4, 7.1, and 7.4 for fully oxidized, one-, two-, three-, and four-electron-reduced proteins, respectively (*13*)]; (iv) the pH dependence is mediated by charged residue(s) readily accessible to the solvent and close to heme I since the largest redox-Bohr cooperativity is observed for this heme, that is, heme I has the strongest pH dependence of its reduction potential (*15*); (v) pH titrations monitored by NMR performed with the *Dv*Hc_3 and the highly homologous ferricytochrome c_3 of *D. vulgaris* Miyazaki also indicate that the protonation center involves at least the propionate group attached to pyrrol carbon number 13 (numbered according to the IUPAC nomenclature), HP-13, of heme I (*9*, *17*). Theoretical studies also suggest that HP-13 of heme I can be the protonation center responsible for the redox-Bohr effect of *Dv*Hc_3 as well as being involved in the positive homotropic cooperativity observed between hemes I and II (*18*). Comparison between the X-ray structure of the oxidized *Dv*Hc_3 (*19*) and the NMR structure obtained for the reduced form (*20*) strongly indicates that the structural motif responsible for the $2e^-/2H^+$ cooperativity involves hemes I and II, the two propionates of heme I, and their interactions with K45 and C46 (Figure 1). The X-ray structure of *Dv*Hc_3 (*19*) shows that the propionate groups of heme I are only partially buried, with HP-17 being more exposed than HP-13. Lysine 45 is located near heme I, establishing a H-bond between its NHδ and propionate 17. Theoretical calculations done on *Dv*Hc_3 suggest that the positive charge of K45 might have a large electrostatic influence on both propionates of heme I and predict that its replacement by noncharged residues such as glycine should significantly increase the pK_a of the redox-Bohr (*18*). In

[†] This work was supported by EU Grants FMRX-CT-98-0218, PRAXIS PCNA BIO/74/96 (AVX), and JCNIT BIA-2164/95 (L.M.S.).

* To whom correspondence should be addressed. Phone: 351-1-4428616. Fax: 351-1-4428766. E-mail: xavier@itqb.unl.pt.

[‡] Universidade Nova de Lisboa.

[§] University of Georgia.

[⊥] Wageningen Agricultural University.

[1] Abbreviations: NOESY, nuclear Overhauser enhancement spectroscopy; HP-13 and HP-17, heme propionates; 12^1CH_3 and 18^1CH_3, heme methyl groups (numbered according to the IUPAC rules); *Dv*Hc_3, *Desulfovibrio vulgaris* (Hildenborough) cytochrome c_3.

S0006-2960(98)01001-0 CCC: $15.00
Published on Web 08/05/1998

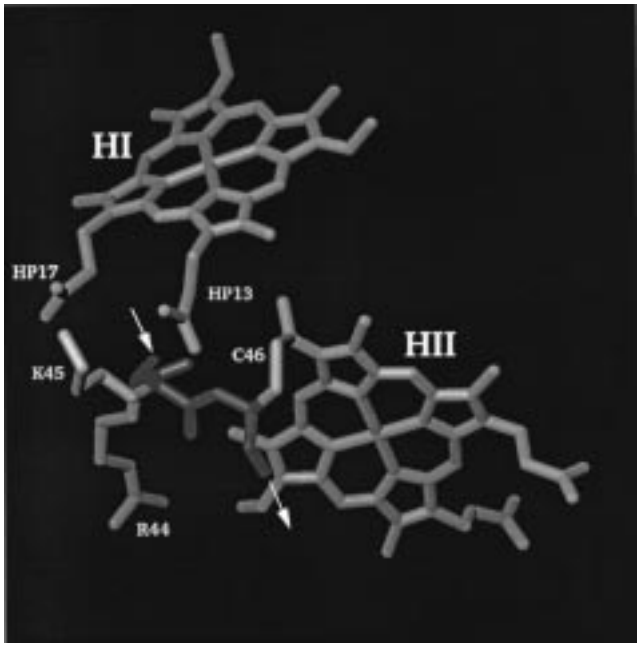

FIGURE 1: Representation of the vicinity of the heme I propionates of *Dv*Hc$_3$. The on-arrow and the off-arrow indicate the start and the end of the polypeptide segment, respectively.

this article, involvement of the propionates of heme I in the redox-Bohr effect is investigated. Therefore, K45 is replaced by uncharged amino acid residues of similar size, to probe their effect in the pK_a of the heme I propionates.

MATERIALS AND METHODS

Reagents. Synthetic oligonucleotides and Elongase^{TR} (used for site-directed mutagenesis) were from Life Science Technologies, restriction endonucleases were from Amersham or Boehringer, and [α-^{35}S]-dATP from Amersham Nucleotide sequencing was with the Thermo Sequenase Cycle Sequencing kit (Amersham).

Site-Directed Mutagenesis and Purification of Mutated Proteins. Plasmid pJ800, containing the gene for *Dv*Hc$_3$ (*21*), was used for site-directed mutagenesis. The codons for K45 and D7 in the cytochrome c_3 gene in pJ800 were replaced by those for Thr, Gln, or Leu and Ala or Asn, respectively, according to a PCR-based mutagenesis method, essentially as described by Landt et al. (*22*). Mutated genes were subcloned into pUC18 and checked by nucleotide sequencing for the presence of the desired mutation and the absence of any unwanted mutations. For the production of mutated cytochromes c_3 proteins, mutated genes were recloned into broad-host-range vector pJRD215 (*23*) and transferred by conjugal transfer from *Escherichia coli* to *Desulfovibrio desulfuricans G200* as described previously (*24*). *D. desulfuricans G200* recombinants were grown in a 30 L fermentor in Starkey's medium (*25*) containing 0.4 mg mL^{-1} kanamycin. Cells from these cultures were harvested by centrifugation, resuspended into 10 mM Tris/HCl, 150 mM NaCl, pH 7.6, and broken in a French Pressure cell (SLM/Aminco) at 8000 psi. Purification of mutated cytochromes c_3 was done as described previously (*24*).

Biochemical and Spectroscopic Characterization of the Mutated DvH Cytochromes c_3. UV−vis spectra were recorded with a Shimadzu UV-360 recording spectrophotometer. Anaerobic visible redox titrations were performed as previously described (*13*), using a 2 μM protein solution in 100 mM MES/BisTris−propane and with the appropriate redox mediators (1 μM). EPR spectroscopy studies were carried out, as in ref *24*, with a Bruker ESP 380 spectrometer equipped with a continuous flow helium cryostat (Oxford Instruments CO.). For the NMR studies, the samples (2 mM) were prepared as previously described (*24*). All ^{1}H two-dimensional spectra were recorded at 297.5 K on a 500 MHz Bruker DRX-500 spectrometer. For protein samples in intermediate stages of oxidation, NOESY experiments were performed using mixing times of 25 ms, a data size of 512 × 2048, and a spectral width of 33 kHz. Chemical shifts are presented in parts per million (ppm) relative to sodium 3-(trimethylsilyl)-(2,2,3,3-$^2H_4$) propane sulfonate, using Tris-(hydroxymethyl)-aminomethane ($C_4H_{11}NO_3$) as an internal reference.

RESULTS

Global Structure and Spectroscopy of the Mutated Cytochromes. The involvement of the heme I propionates in the redox-Bohr effect was studied by replacing K45, which forms a salt bridge with HP-17, by uncharged amino acids. When K45 is replaced by threonine or glutamine, stable proteins are produced which can be purified with similar yields (0.25 mg of protein/g of wet-weight cells) as the wild-type protein expressed in *D. desulfuricans* G200 (*24*, *26*). Purified wild-type and mutated proteins all had a highly similar purity coefficient ($[(A_{553red} - A_{570red})/A_{280ox}] = 2.9$) and identical UV−vis spectra, in both the oxidized and reduced forms (data not shown). In contrast, replacement of K45 by leucine resulted in very low yields of the mutated protein, which rapidly denaturated and did not allow further study.

No major differences are observed in the EPR spectra of wild-type and K45T- and K45Q-mutated ferricytochrome c_3. Table 1 shows the g values obtained by simulation of the experimental data according to Campos (*27*).

2D NMR results of the reduced K45T- and K45Q-mutated cytochromes (data not shown) revealed that the interheme NOESY cross-peaks network, which involves heme methyls, heme thioether methyl groups, and meso protons, is identical to that observed for the wild-type protein (*29*).

EPR and NMR data indicate that removal of the salt bridge between K45 and HP-17 in the K45T- and K45Q-mutated proteins does not cause a significant rearrangement of the architecture of the heme core, the overall folding of the proteins, or the electronic structure around the heme irons. However, the apolar side chain of leucine is not tolerated in this position.

Also, the putative involvement of another residue close to heme I, D7, in the redox-Bohr effect was tested by replacement of this residue by alanine and asparagine. However, these mutations did not allow the production of stable holoprotein. Failure to produce D7A- and D7N-mutated cytochromes c_3 suggests that the network of hydrogen bonds provided by the carboxylate group of D7 (to the peptidyl NH group and hydroxyl side chain of S23 (*19*)) is structurally important for the appropriate folding around heme I.

Table 1: EPR g values for the Wild-Type and Mutated *Dv*Hc_3

	g_z, g_y, g_x			
	heme I	heme II	heme III	heme IV
*Dv*Hc_3 K45 (*27*)	2.96, 2.31, 1.44	3.14, 2.30, 1.07	2.80, 2.31, 1.64	2.99, 2.30, 1.56
*Dv*Hc_3 K45T	2.97, 2.28, 1.44	3.14, 2.30, 1.07[a]	2.83, 2.31, 1.64	2.98, 2.30, 1.56
*Dv*Hc_3 K45Q	2.96, 2.29, 1.44	3.14, 2.30, 1.07[a]	2.83, 2.31, 1.64	2.99, 2.30, 1.56

[a] g_x not observed, determined by $\sum g_i^2 = 16$ (*28*).

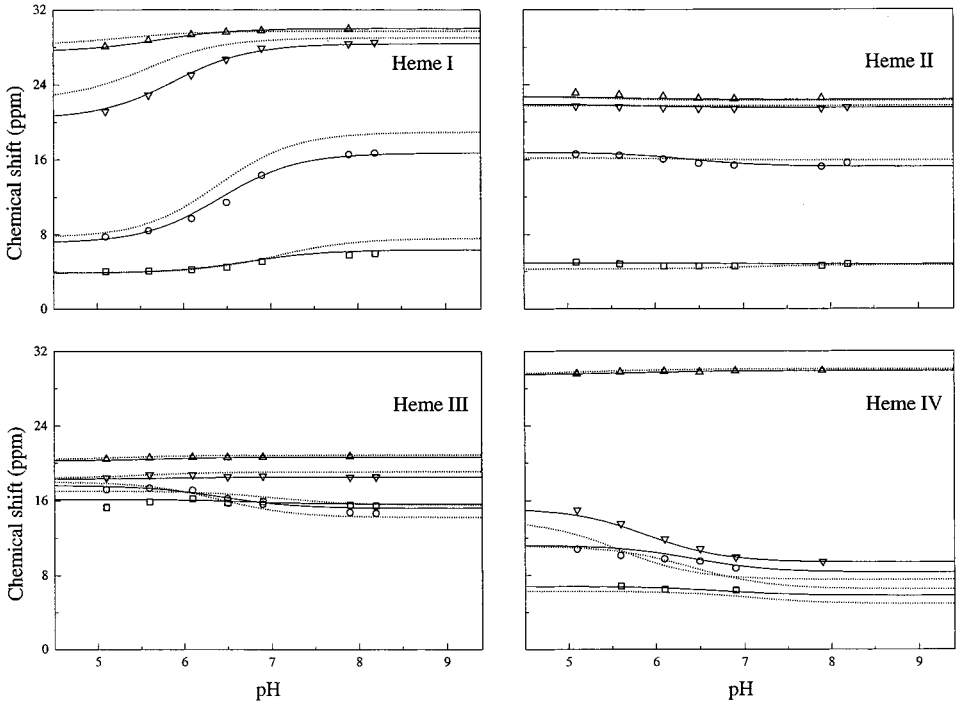

FIGURE 2: Chemical shift pH dependence of the heme methyl group resonances $18^1CH_3^I$, $18^1CH_3^{II}$, $12^1CH_3^{III}$, and $18^1CH_3^{IV}$ of K45T *Dv*H cytochrome c_3. Squares correspond to stage 1 of oxidation, circles to stage 2, downward-pointing triangles to stage 3, and upward-pointing triangles to stage 4. The full lines represent the best fit (rmsd = 0.50 ppm) of the shifts for the mutated *Dv*H cytochromes c_3 to the model of five interacting centers using the energy parameters listed in Table 2. Dotted lines represent the best fit for the wild-type *Dv*Hc_3 (*13*, *17*).

The Redox-Bohr Effect in Wild-Type and K45-Mutated Cytochromes c_3. The redox properties of the mutated cytochromes c_3 were analyzed by monitoring one methyl group of each heme ($18^1CH_3^I$, $18^1CH_3^{II}$, $12^1CH_3^{III}$, and $18^1CH_3^{IV}$) during an NMR redox titration performed as previously reported (*15*, *30*). Under the experimental conditions used, the intermolecular electron exchange is slow on the NMR time scale so that separate peaks are observed for each oxidation stage. Each heme methyl resonance was then traced from the different oxidation stages throughout each one-electron reduction step, back to its resonance in the fully reduced protein (*13*, *24*). The chemical shifts of the methyl groups at intermediate oxidative levels were obtained from NOESY spectra (Figures 2 and 3).

The pH dependence of the observed paramagnetic shifts of the four heme methyl groups for both mutated cytochromes was fitted within the framework of a model which considers five interacting centers: four hemes and one ionizable center (*13*, *15*) (Figures 2 and 3). The pH range was chosen in order to minimize any contribution from additional ionizations that can occur at extreme pH values, outside the physiological pH range (*13*).

UV−vis titrations performed at two pH values (pH = 6.6 and 8.0) were used for calibration of the microscopic redox potentials and heme redox interaction energies which were obtained by fitting the chemical shift data for both mutated cytochromes (*13*, *17*). This allowed the determination of the absolute redox parameters for K45T and K45Q cytochromes, which are shown in Table 2.

The NMR data show that replacement of K45 induced some changes in the cooperativities. For K45T cytochrome c_3, the redox-Bohr interactions between the ionizable center and both hemes I and II weakened, causing small alterations in the macroscopic pK_a values of the various oxidation stages for this mutant, when compared with those of the wild-type cytochrome (Table 3). Altogether, there was a small decrease of the redox potentials of the hemes and a decrease of 0.8 units in the global ΔpK_a ($pK_a^{red} - pK_a^{ox}$, i.e., total redox-Bohr effect).

Significantly, for K45Q cytochrome c_3 the heterotropic cooperativities were quite altered. Although the pK_a^{ox} is maintained, the pK_a values for all four other redox states increased, showing a rise of ~2 units for the global pK_a (Table 3). No major alterations were observed in the heme redox potentials, but a much lower value of the homotropic cooperativity between hemes I and II was measured (−1 meV). Both in the wild-type and in the K45T cytochrome c_3, the second and third hemes to be oxidized, hemes II and I, have a stronger positive homotropic cooperativity (−40 meV). This is reflected by the fact that the observed

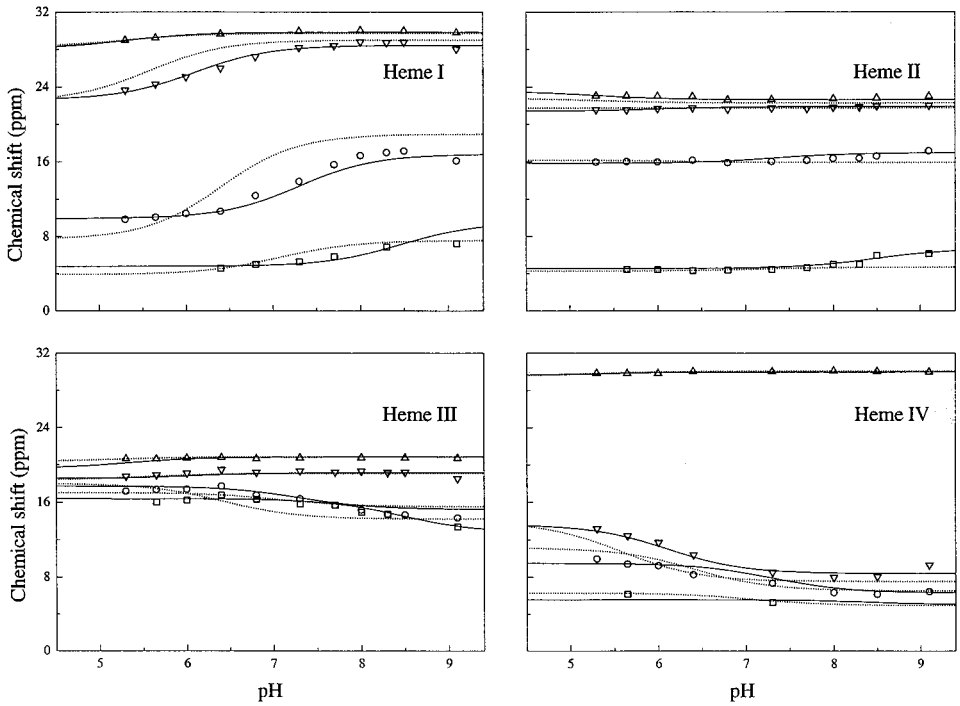

FIGURE 3: Chemical shift pH dependence of the heme methyl group resonances of K45Q cytochrome c_3. The heme methyl group resonances and legend details are the same as that of Figure 2.

Table 2: Energy Parameters Calculated Using a Model of Five Interacting Centers Fitted to the NMR and Visible Data[a]

	energies (meV)				
	heme I	heme II	heme III	heme IV	ionizable center
*Dv*Hc$_3$ K45 (*13*)					
heme I	**−245**	−43	20	−4	−70
heme II		**−267**	−8	8	−30
heme III			**−334**	32	−18
heme IV				**−284**	−6
ionizable center					**439**
*Dv*Hc$_3$ K45T					
heme I	**−229**	−42	15	0	−51
heme II		**−263**	−6	5	−9
heme III			**−318**	29	−9
heme IV				**−274**	−2
ionizable center					**410**
*Dv*Hc$_3$ K45Q					
heme I	**−273**	−1	32	14	−84
heme II		**−276**	6	23	−74
heme III			**−341**	43	−37
heme IV				**−283**	−40
ionizable center					**548**

[a] As described in ref *13*. Diagonal elements (boldface) represent the energy for oxidizing the hemes (standard errors of 5 meV) and deprotonating the ionizable group in the fully reduced molecule. The off-diagonal elements represent the energies of redox and redox-Bohr interactions upon oxidation and deprotonation, respectively (standard errors of 3 meV).

paramagnetic shift of $12CH_3^{III}$ in oxidation stage 2 is smaller than in stage 1, at neutral and high pH. For K45Q cytochrome c_3 the observed paramagnetic shift of $12^1CH_3^{III}$ in stage 2 is no longer smaller than in stage 1. Nevertheless, the same order of oxidation was observed, and the ability to couple proton transfer with a proton-assisted concerted two-electron transfer is maintained (Figure 4). In fact, although the magnitude of the positive redox interaction has decreased, it is still sufficient to cancel the negative contribution from the electrostatic interaction.

Table 3: pK_a Values of the Wild-Type and Mutated *Dv*Hc$_3$ in the Different Oxidation Stages[a]

	pK_a		
stage	*Dv*Hc$_3$ K45 (*13*)	*Dv*Hc$_3$ K45T	*Dv*Hc$_3$ K45Q
0	7.4	6.9	9.3
1	7.1	6.7	8.5
2	6.4	6.4	7.3
3	5.6	5.9	6.1
4	5.3	5.7	5.3
ΔpK_a	2.1	1.2	4.0

[a] The stages are numbered from 0 (fully reduced) to 4 (fully oxidized), according to the number of oxidized hemes.

Conformational Differences between Wild-Type and Mutated Cytochromes c_3. The changes in the NMR chemical shifts caused by nearby aromatic rings (ring current shifts) were used to probe conformational changes of the amino acid segment comprising residues 44−46 between the wild-type (*20*) and the mutated cytochromes c_3. These residues are close both to heme II and to the propionate groups of heme I. When K45T cytochrome c_3 is compared with the wild-type cytochrome, no major differences are observed. Also, the ring current shifts of R44 are similar in wild-type and in K45Q cytochromes c_3. However, the contributions of the ring currents to the chemical shifts of the Hα of residue 45 and the Hβ of C46 are higher in the K45Q mutated protein than in the wild-type protein (0.3 and 0.1 ppm, respectively, cf. Table 4). As the ring current shifts on these protons are dominated by the contribution of heme II, this increase indicates that the backbone of these residues becomes more buried in the mutated cytochrome, moving toward heme II. This conclusion is supported by the observation that the intensity of the NOE cross-peak between the Hα of Q45 and the meso15 proton of heme I decreases, while the cross-peaks between the Hα protons of heme I HP-13 and those of its methyl 12^1 become more intense. These results

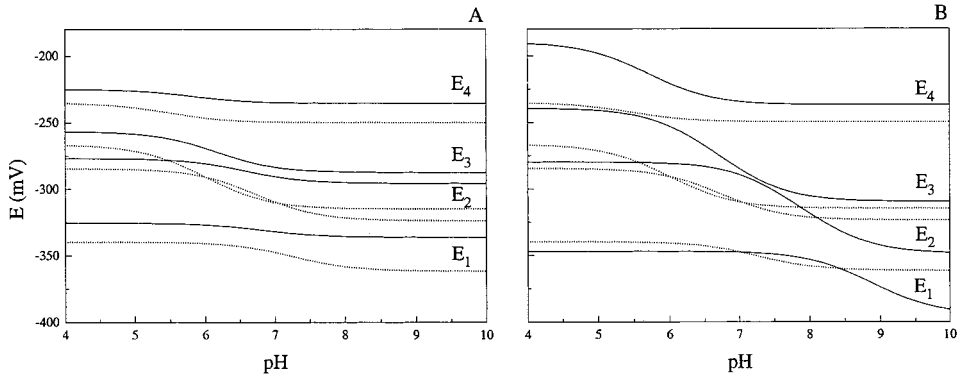

FIGURE 4: Macroscopic reduction potentials of the four oxidation stages for K45T (A) and K45Q (B) *Dv*H cytochromes c_3 calculated as a function of pH from the energy parameters listed in Table 2. Dotted lines represent the macroscopic reduction potentials for the wild-type *Dv*Hc_3 (*13*).

Table 4: Chemical Shifts and Ring Currents (ppm) of the Assigned Protons in the Fully Reduced Form of the Wild-Type and Mutated *Dv*H Cytochromes c_3

	residue R44				residue X45	residue C46	
	Hα	Hβ^a	Hγ^a	Hδ	Hα	Hα	Hβ
			Chemical Shifts (ppm)				
*Dv*Hc_3 K45 (*20*)	4.85	1.93	1.58	3.29	4.95	4.99	2.47
*Dv*Hc_3 K45T	4.91	1.93	1.63	3.31	4.96	4.97	2.46
*Dv*Hc_3 K45Q	4.89	1.98	1.63	3.34	5.28	5.03	2.57
			Ring Currents (ppm)				
*Dv*Hc_3 K45 (*20*)	0.51	0.17	−0.05	0.09	0.63	0.28	−0.65
*Dv*Hc_3 K45T	0.57	0.12	0.00	0.11	0.64	0.26	−0.67
*Dv*Hc_3 K45Q	0.56	0.17	0.00	0.14	0.96	0.32	−0.56

[a] Average values.

indicate that the movement of the polypeptide chain between 44 and 46 toward the interior of the protein induces a conformational alteration of HP-13 propionate of heme I, to maintain the H-bond of the carboxylate group to the main chain NH of C46, the cysteinyl ligation of heme II.

DISCUSSION

The analysis of the thermodynamic parameters obtained for the mutated cytochromes clearly shows that replacement of K45 affects the homotropic and heterotropic cooperativities. The observed modifications may result from several simultaneous effects: (i) the different H-bond capability of the new amino acid residues when compared with K45; (ii) the different solvent accessibility for heme I propionates; (iii) the removal of the positive charge near the carboxylate groups of the propionates, which should cause an increase of the pK_a values; and (iv) the local conformational changes.

The data obtained for the mutated proteins show that, in general, the absence of the positive charge of K45 altered the pK_a values, although to a different extent depending on the redox state of the protein (Table 3). The pK_a^{ox} for K45Q cytochrome c_3 is identical to that of the wild-type cytochrome, while a slightly higher value for K45T (∼0.4 pK_a units) is observed. In the mutated cytochromes, the effect of removing the positive charge of K45 seems to be canceled by an increase in the solvent exposure of the propionate groups. This effect is more pronounced in K45Q than in K45T. In the absence of redox-linked conformational changes, replacement of residue 45 by uncharged residues should modify the pK_a^{ox} and pK_a^{red} values in a similar way. However, as previously reported for the wild-type cytochrome c_3 (*20*), reduction leads to a movement of the polypeptide chain between residue 44 and residue 47 toward the propionate edge of heme I. In fact, for K45Q cytochrome c_3 the alterations detected in the NMR spectra of the reduced state indicate that the HP-13 of heme I becomes even more protected in this mutant, explaining the much higher value for its pK_a^{red} (∼2 pK units) when compared to the pK_a^{red} of the wild-type cytochrome. This effect is supported by the NOE and ring current effects described above. On the contrary, although for the reduced form of K45T the NMR structural parameters are similar to those of the wild-type ferrocytochrome, a decrease in the pK_a^{red} (∼0.5) for this mutant occurred, suggesting that in this case the propionates of heme I become more exposed in the reduced state.

Although several effects occur simultaneously, the data show that the nature of residue 45 influences the pK_a of the propionate groups and, more importantly, support the hypothesis that heme I propionates and their neighboring residues control the redox-Bohr effect observed for *Dv*Hc_3.

The local arrangement of charged groups in the vicinity of heme propionates may be a more general motif for coupling the transfer of electrons and protons. In fact, comparison of *Dv*Hc_3 with bovine and *Paracoccus denitrificans* cytochrome oxidases (*31*−*33*) shows that the architectures of the heme cores have interesting similarities which may justify some speculation (*24*). In cytochrome oxidase a charged residue, R473, forms a hydrogen bond with a propionate group of heme a_3 and is followed by R474, while in *Dv*Hc_3 there is an equivalent hydrogen bond between a propionate group of heme I and K45, which is preceded by R44. In both proteins electron transfer is coupled to proton transfer, and the fact that a similar arrangement around the redox centers is observed may be more than just a coincidence.

ACKNOWLEDGMENT

We are indebted to Prof. G. Voordouw for providing the pJ800 vector, Dr. J. Wall for the *D. desulfuricans* G200 strain, Prof. M. Teixeira for his help with the EPR studies, J. Carita and the Fermentation Plant at the ITQB/IBET for growing the bacterial cells, I. Pacheco for technical collaboration, and Dr. C. Soares for helpful discussions.

REFERENCES

1. Papa, S., Guerrieri, F., and Izzo, G. (1979) *FEBS Lett. 105*, 213−216.
2. Losada, M., Hervas, M., de la Rosa, M. A., and de la Rosa, F. F. (1983) *Bioelectrochem. Bioenerg. 6*, 205−225.
3. Xavier, A. V. (1986) *J. Inorg. Biochem. 28*, 239−243.
4. Pettigrew, G. W., Bartsch, R. G., Meyer, T. E., and Kamen, M. D. (1978) *Biochim. Biophys. Acta 503*, 509−523.
5. Moore, G. R., Pettigrew, G. W., Pitt, R. C., and Williams, R. J. P. (1980) *Biochim. Biophys. Acta 590*, 261−271.
6. Barakat, R., and Strekas, T. C. (1982) *Biochim. Biophys. Acta 679*, 393−399.
7. Moore, G. R., Harris, D. E., Leitch, F. A., and Pettigrew, G. W. (1984) *Biochim. Biophys. Acta 764*, 331−342.
8. Leitch, F. A., Moore, G. R., and Pettigrew, G. W. (1984) *Biochemistry 23*, 1831−1838.
9. Park, J. S., Ohmura, T., Kano, K., Sagara, T., Niki, K., Kyoguku, Y., and Akutsu, H. (1996) *Biochim. Biophys. Acta 1293*, 45−54.
10. Cutruzzola, F., Ciabatti, I., Rolli, G., Falcinelli, S., Arese, M., Ranghino, G., Anselmino, A., Zennaro, E., and Silvestrini, M. C. (1997) *Biochem. J. 322*, 35−42.
11. Coutinho, I. B., and Xavier, A. V. (1994) *Methods Enzymol. 243*, 119−140.
12. Coutinho, I. B., Turner, D. L., LeGall, J., and Xavier, A. V. (1995) *Eur. J. Biochem. 230*, 1007−1013.
13. Turner, D. L., Salgueiro, C. A., Catarino, T., LeGall, J., and Xavier, A. V. (1996) *Eur. J. Biochem. 241*, 723−731.
14. Louro, R. O., Pacheco, I., Turner, D. L., LeGall, J., and Xavier, A. V. (1996) *FEBS Lett. 390*, 59−62.
15. Turner, D. L., Salgueiro, C. A., Catarino, T., LeGall, J., and Xavier, A. V. (1994) *Biochim. Biophys. Acta 1187*, 232−235.
16. Louro, R. O., Catarino, T., Salgueiro, C. A., LeGall, J., and Xavier, A. V. (1996) *J. Biol. Inorg. Chem. 1*, 34−38.
17. Salgueiro, C. A., Turner, D. L., and Xavier, A. V. (1997) *Eur. J. Biochem. 244*, 721−734.
18. Soares, C. M., Martel, P. J., and Carrondo, M. A. (1997) *J. Biol. Inorg. Chem. 2*, 714−727.
19. Matias, P. M., Frazão, C., Morais, J., Coll, M., and Carrondo, M. A. (1993) *J. Mol. Biol. 234*, 680−699.
20. Messias, A. C., Kastrau, D. H. W., Costa, H. S., LeGall, J., Turner, D. L., Santos, H., and Xavier, A. V. (1998) *J. Mol. Biol.* (in press).
21. Voordouw, G., and Brenner, S. (1986) *Eur. J. Biochem. 159*, 347−351.
22. Landt, O., Grunert, H. P., and Hahn, U. (1990) *Gene 96*, 125−128.
23. Davison, J., Heusterspreute, M., Chevalier, N., Vihn, H. T., and Brunel, F. (1987) *Gene 51*, 275−280.
24. Saraiva, L. M., Salgueiro, C. A., LeGall, J., van Dongen, W. M. A., and Xavier, A. V. (1996) *J. Biol. Inorg. Chem. 1*, 542−550.
25. Starkey, R. L. (1938) *Arch. Mikrobiol. 8*, 268−304.
26. Voordouw, G., Pollock, W. B. R., Bruschi, M., Guerlesquin, F., Rapp-Giles, B. J., and Wall, J. D. (1990) *J. Bacteriol. 172*, 6122−6126.
27. Campos, A. (1994) Ph.D. Thesis, FCT, Universidade Nova de Lisboa.
28. Taylor, C. P. S. (1977) *Biochim. Biophys. Acta 491*, 137−149.
29. Turner, D. L., Salgueiro, C. A., LeGall, J., and Xavier, A. V. (1992) *Eur. J. Biochem. 210*, 931−936.
30. Louro, R. O., Catarino, T., LeGall, J., and Xavier, A. V. (1997) *J. Biol. Inorg. Chem. 2*, 488−491.
31. Iwata, S., Ostermeier, C., Ludwig, B., and Michel, H. (1995) *Nature 376*, 660−669.
32. Tsukihara, T., Aoyama, H., Yamashita, E., Tomizaki, T., Yamaguchi, H., Shinzawa-Itoh, K., Nakashima, R., Yaono, R., and Yoshikawa, S. (1995) *Science 269*, 1069−1074.
33. Tsukihara, T., Aoyama, H., Yamashita, E., Tomizaki, T., Yamaguchi, H., Shinzawa-Itoh, K., Nakashima, R., Yaono, R., and Yoshikawa, S. (1996) *Science 272*, 1136−1144.

BI981001V